Soft Soils Improved by Prefabricated Vertical Drains: Performance and Prediction

B. Indraratna, C. Rujikiatkamjorn, X.-Y. Geng, G. McIntosh, R. Kelly

Abstract. The use of prefabricated vertical drains with vacuum preloading and surcharge preloading is now common practice and is proving to be one of the most effective ground improvement techniques known. The factors affecting its performance, such as the smear zone, the drain influence zone, and drain unsaturation, are discussed in this paper. In order to evaluate these effects a large scale consolidation test was conducted and it was found that the proposed Cavity Expansion Moreover, the procedure for converting an equivalent 2-D plane strain multi-drain analysis that considers the smear zone and vacuum pressure are also described. The conversion procedure was incorporated into finite element codes using a modified Cam-clay theory. Numerical analysis was conducted to predict excess pore pressure and lateral and vertical displacement. Three case histories are analyzed and discussed, including the sites of Muar clay (Malaysia), the Second Bangkok International Airport (Thailand), and the Sandgate railway line (Australia). The predictions were then compared with the available field data, which include settlement, excess pore pressure, and lateral displacement. Further findings verified that smear, drain unsaturation, and vacuum distribution can significantly influence consolidation so they must be modeled appropriately in any numerical analysis to obtain reliable predictions.

Keywords: analytical model, cyclic loading, numerical model, soft soils, vacuum preloading, vertical drains.

1. Introduction

Preloading of soft clay with vertical drains is one of the most popular methods used to increase the shear strength of soft soil and control its post-construction settlement. Since the permeability of soils is very low, consolidation time to the achieved desired settlement or shear strength may take too long (Holtz, 1987; Indraratna *et al.*, 1994). Using prefabricated vertical drains (PVDs), means that the drainage path is shortened from the thickness of the soil layer to the radius of the drain influence zone, which accelerates consolidation (Hansbo, 1981). This system has been used to improve the properties of foundation soil for railway embankments, airports, and highways (Li & Rowe, 2002).

Over the past three decades the performance of various types of vertical drains, including sand drains, sand compaction piles, prefabricated vertical drains (geosynthetic) and gravel piles, have been studied. Kjellman (1948) introduced prefabricated band shaped drains and cardboard wick drains for ground improvement. Typically, prefabricated band drains consist of a plastic core with a longitudinal channel surrounded by a filter jacket to prevent clogging. Most vertical drains are approximately 100 mm wide and 4 mm thick.

To study consolidation due to PVDs, unit cell analysis with a single drain surrounded by a soil cylinder has usually been proposed (*e.g.* Barron, 1948; Yoshikuni & Nakanodo, 1974). PVDs under an embankment not only accelerate consolidation, they also influence the pattern of subsoil deformation. At the centre line of an embankment where lateral displacement is negligible, unit cell solutions are sufficient but elsewhere, especially towards the embankment toe, any prediction from a single drain analysis is not accurate enough because of lateral deformation and heave (Indraratna *et al.*, 1997).

Figure 1 shows the vertical cross section of an embankment stabilised by a vertical drain system, with the instruments required to monitor the soil foundation. Before PVDs are installed superficial soil must be removed to ease the installation of the horizontal drainage, the site must be graded, and a sand platform compacted. The sand blanket drains water from the PVDs and supports the vertical drain installation rigs.

Figure 2 illustrates a typical embankment subjected to vacuum preloading (membrane system). Where a PVD system is used with vacuum preloading, horizontal drains must be installed after a sand blanket has been put in place (Cognon *et al.*, 1994). The horizontal drains are connected to a peripheral Bentonite slurry trench, which is then sealed

B. Indraratna, PhD, Professor and Head, School of Civil, Mining & Environmental Engineering, Director, Centre for Geomechanics & Railway Engineering, University of Wollongong, Wollongong City, NSW 2522, Australia. e-mail: indra@uow.edu.au.
C. Rujikiatkamjorn, PhD, Senior Lecturer, Centre for Geomechanics & Railway Engineering, School of Civil, Mining and Environmental Engineering, Faculty of Engineering, University of Wollongong, Wollongong City, NSW 2522, Australia. e-mail: cholacha@uow.edu.au.
X.-Y. Geng, PhD, Research Fellow, Centre for Geomechanics & Railway Engineering, School of Civil, Mining and Environmental engineering, Faculty of Engineering, University of Wollongong, Wollongong City, Australia. e-mail: xgeng@uow.edu.au.
G. McIntosh, BEng, MEng, Principal Engineer, Douglas Partners Pty Ltd, Unanderra, NSW Australia. e-mail: Geoff.McIntosh@douglaspartners.com.au.
R. Kelly, PhD, Associate Engineer, Coffey Geotechnics, Sydney, Australia. e-mail: Richard_Kelly@coffey.com.
Submitted on November 1, 2010; Final Acceptance on December 15, 2011; Discussion open until July 31, 2012.

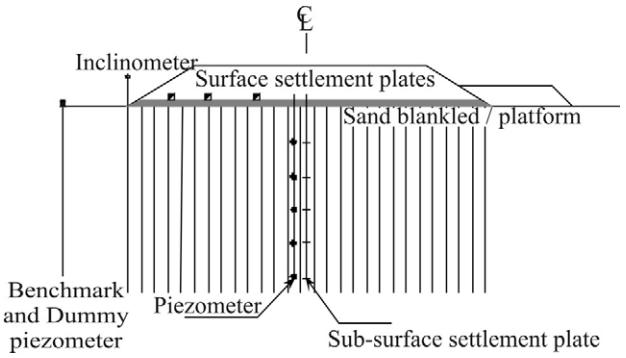

Figure 1 - Vertical drain system with preloading.

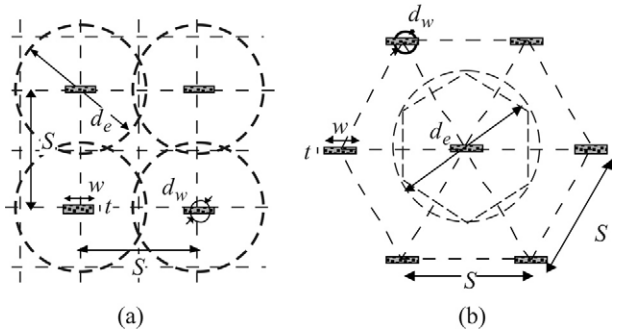

Figure 3 - Drain installation pattern (a) square pattern; (b) triangular pattern.

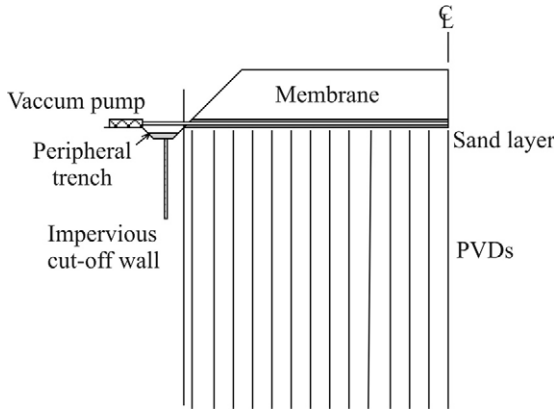

Figure 2 - Vacuum preloading system.

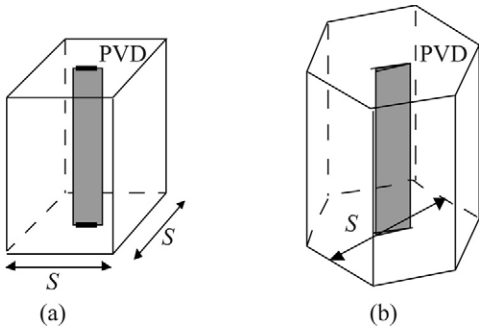

Figure 4 - Vertical drain and its dewatered soil zone (a) unit cell with square grid installation and (b) unit cell with triangular grid installation.

with an impermeable membrane and cut-off walls to prevent possible vacuum loss at the embankment edges. The vacuum pumps are connected to the discharge module extending from the trenches. The vacuum generated by the pump increases the hydraulic gradient towards the drain which accelerates the dissipation of excess pore water pressure.

2. Factors Influencing The Performance of A Vacuum Or Surcharge Preloading With Consolidated Pvds

2.1. Equivalent drain diameter and drain influence zone

As shown in Fig. 3, PVDs with a rectangular cross section are usually installed in a triangular or square pattern. Their shapes are not the same as the circular cross section considered in the unit cell theory so a PVD with a polygon influence zone must be transformed into a cylindrical drain with a circular influence zone (Fig. 4). The approximate equations proposed for the equivalent drain diameter are based on various hypotheses, hence the different results. The formulations for an equivalent cylindrical drain conversion available from previous studies are highlighted below:

$$d_w = \frac{2(w+t)}{\pi} \quad \text{(Hansbo, 1979)} \tag{1}$$

$$d_w = \frac{(w+t)}{2} \quad \text{(Atkinson \& Eldred, 1981)} \tag{2}$$

$$d_w = 0.5w + 0.7t \quad \text{(Long \& Covo, 1994)} \tag{3}$$

where d_w = equivalent PVDs diameter and w and t = width and thickness of the PVD, respectively.

2.2. Smear zone

The smear zone is the disturbance that occurs when a vertical drain is installed using a replacement technique. Because the surrounding soil is compressed during installation there is a substantial reduction in permeability around the drain, which retards the rate of consolidation. In this section the Elliptical Cavity Expansion Theory was used to estimate the extent of the smear zone (Ghandeharioon *et al.* 2009; Sathananthan *et al.* 2008). This prediction was then compared with laboratory results based on permeability and variations in the water content. The detailed theoretical developments are explained elsewhere by Cao *et al.* (2001) and Ghandeharioon *et al.* (2009), so only a brief summary is given below. The yielding criterion for soil obeying the MCC model is:

$$\eta = M\sqrt{\frac{p'_c}{p'} - 1} \quad (4)$$

where p'_c = the stress representing the reference size of yield locus, p' = mean effective stress, M = slope of the critical state line and η = stress ratio. Stress ratio at any point can be determined as follows:

$$\ln\left(1 - \frac{(a^2 - a_0^2)}{r^2}\right) = -\frac{2(1+\nu)}{3\sqrt{3}(1-2\nu)}\frac{\kappa}{\upsilon}\eta - 2\sqrt{3}\,\frac{\kappa\Lambda}{\upsilon M} f(M, \eta, \mathrm{OCR}) \quad (5)$$

$$f(M, \eta, \mathrm{OCR}) = \frac{1}{2}\ln\left[\frac{(M+\eta)(1-\sqrt{\mathrm{OCR}-1})}{(M-\eta)(1+\sqrt{\mathrm{OCR}-1})}\right] - \tan^{-1}\left(\frac{\eta}{M}\right) + \tan^{-1}(\sqrt{\mathrm{OCR}-1}) \quad (6)$$

In the above expression, a = radius of the cavity, a_0 = initial radius of the cavity, ν = Poisson's ratio, κ = slope of the over consolidation line, υ = specific volume, OCR = over consolidation ratio and λ is the slope of the normal consolidation line).

Figure 5 shows the variation of the permeability ratio (k_h/k_v), obtained from large scale laboratory consolidation and predicted plastic shear strain along the radius. Here the radius of the smear zone was approximately 2.5 times the radius of the mandrel, which agreed with the prediction using the cavity expansion theory.

2.3. Drain unsaturation

Due to an air gap from withdrawing the mandrel, and dry PVDs, unsaturated soil adjacent to the drain can occur. The apparent delay in pore pressure dissipation and consolidation can be observed during the initial stage of loading (Indraratna *et al.*, 2004). Figure 6 shows how the top of the drain takes longer to become saturated than the bottom. Figure 6 illustrates the change in degree of saturation with the depth of the drain. Even for a drain as short as 1 m, the time lag for complete drain saturation can be significant.

2.4. The effect of vacuum consolidation on the lateral yield of soft clays

In order to investigate the effect of a combined vacuum and surcharge load on lateral displacement, a simplified plane strain (2-D) finite element analysis could be used (Indraratna *et al.* 2008). The outward lateral compressive strain due to surcharge can be reduced by applying suction (vacuum preloading). The optimisation of vacuum and surcharge preloading pressure to obtain a given settlement must be considered in any numerical model to minimise lateral displacement at the embankment toe (Fig. 7a), while identifying any tension zones where the vacuum pressure may be excessive.

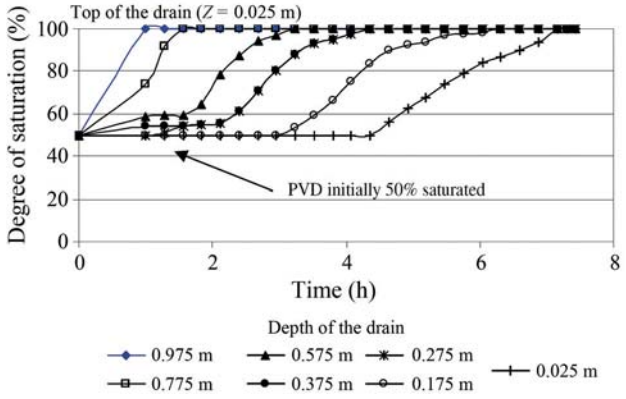

Figure 6 - Degree of drain saturation with time (after Indraratna *et al.* 2004).

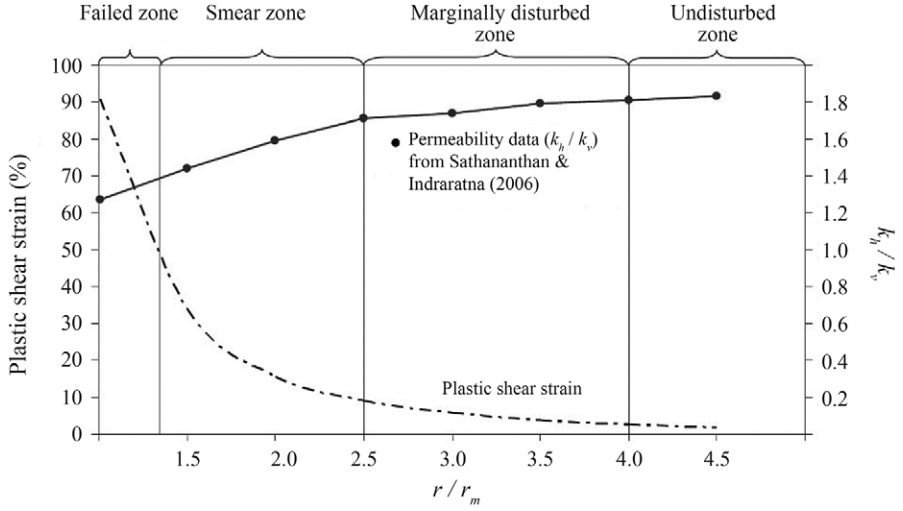

Figure 5 - Variations in the ratio of the horizontal coefficient of permeability to the vertical coefficient of permeability and the plastic shear strain in radial direction (adopted from Ghandeharioon *et al.* 2009).

As expected, the vacuum pressure alone can create inward lateral movement, whereas preloading without any vacuum may contribute to an unacceptable outward lateral movement. The particular situations for most clays is generally a combination of 40% surcharge preloading stress with a 60% vacuum, which seems to maintain a lateral displacement close to zero. Figure 7b presents the various profiles of surface settlement with an increasing surcharge loading. A vacuum alone may generate settlement up to 10 m away from PVD treated boundary while the application of VP can minimise the value of soil heave beyond the embankment toe.

3. Equivalent Plane Strain For Multi-Drain Analysis

In order to reduce the calculation time, most available finite element analyses on embankments stabilised by PVDs are based on a plane strain condition. To obtain a realistic 2-D finite element analysis for vertical drains, the equivalence between a plane strain condition and an in-situ axisymmetric analysis needs to be established. Indraratna and Redana (2000); Indraratna *et al.* (2005) converted the unit cell of a vertical drain shown in Fig. 8 into an equivalent parallel drain well by determining the coefficient of permeability of the soil.

By assuming that the diameter of the zone of influence and the width of the unit cell in a plane strain to be the same, Indraratna & Redana (2000) presented a relationship between k_{hp} and k'_{hp}, as follows:

$$k_{hp} = \frac{k_h\left[\alpha+\beta\frac{k_{hp}}{k'_{hp}}+\theta(2lz-z^2)\right]}{\left[\ln\left(\frac{n}{s}\right)+\left(\frac{k_h}{k'_h}\right)\ln(s)-0.75+\pi(2lz-z^2)\frac{k_h}{q_w}\right]} \quad (7)$$

In Eq. (7), if well resistance is neglected, the smear effect can be determined by the ratio of the smear zone permeability to the undisturbed permeability, as follows:

$$\frac{k'_{hp}}{k_{hp}} = \frac{\beta}{\frac{k_{hp}}{k_h}\left[\ln\left(\frac{n}{s}\right)+\left(\frac{k_h}{k'_h}\right)\ln(s)-0.75\right]-\alpha} \quad (8)$$

$$\alpha = \frac{2}{3}-\frac{2b_s}{B}\left(1-\frac{b_s}{B}+\frac{b_s^2}{3B^2}\right) \quad (8a)$$

$$\beta = \frac{1}{B^2}(b_s-b_w)^2+\frac{b_s}{3B^2}(3b_w^2-b_s^2) \quad (8b)$$

$$\theta = \frac{2k_{hp}^2}{k'_{hp}q_zB}\left(1-\frac{b_w}{B}\right) \quad (8c)$$

where k_{hp} and k'_{hp} are the undisturbed horizontal and the corresponding smear zone equivalent permeability, respectively.

The simplified ratio of plane strain to axisymmetric permeability by Hird *et al.* (1992) is readily obtained when the effect of smear and well resistance are ignored in the above expression, as follows:

$$\frac{k_{hp}}{k_h} = \frac{0.67}{[\ln(n)-0.75]} \quad (9)$$

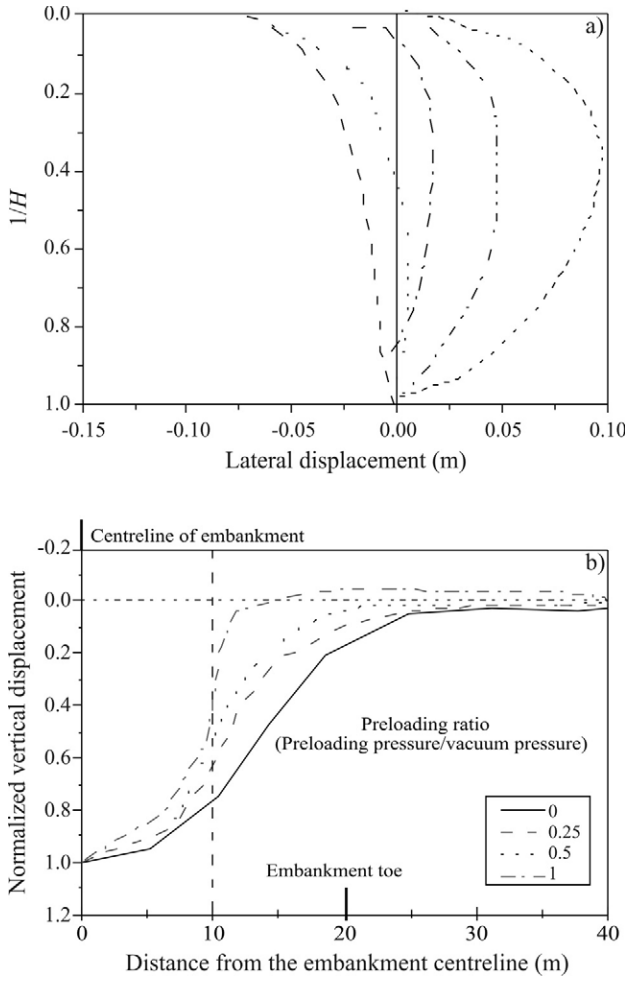

Figure 7 - (a) Lateral displacements; and (b) surface settlement profiles (Indraratna *et al.* 2008).

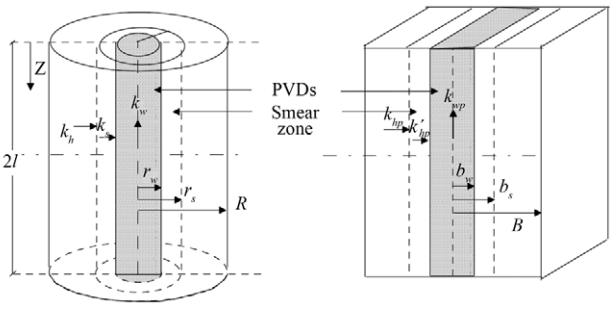

Figure 8 - Conversion of an axisymmetric unit cell into plane strain condition (after Indraratna & Redana 2000).

The well resistance is derived independently and yields an equivalent plane strain discharge capacity of drains, which can be determined from the following equation:

$$q_z = \frac{2}{\pi B} q_w \quad (10)$$

With vacuum preloading, the equivalent vacuum pressures in plane strain and axisymmetric are the same.

4. Application To Case Histories

4.1. Muar clay embankment

One of the test embankments on Muar plain was constructed to failure. The failure was due to a "quasi slip circle" type of rotational failure at a critical embankment height at 5.5 m, with a tension crack propagating through the crust and the fill layer (Fig. 9). Indraratna *et al.* (1992) analysed the performance of the embankment using a finite element Plane strain finite element analysis employing two distinct constitutive soil models, namely, the Modified Cam-clay theory using the finite element program CRISP (Woods, 1992) and the hyperbolic stress-strain behaviour using the finite element code ISBILD (Ozawa & Duncan, 1973). Two modes of analysis were used, undrained and coupled consolidation. Undrained analysis was used when the loading rate was much faster than the dissipation rate of excess pore pressure. This will cause excess pore pressure to build up during loading but will not alter the volume. While excess pore pressure is generated simultaneously with drainage, a positive or negative change in volume is allowed for coupled consolidation analysis.

The essential soil parameters used for the Modified Cam-clay model are summarised in Table 1 and a summary of soil parameters for undrained and drained analyses by ISBILD is tabulated in Table 2. Because properties of a topmost crust were not available it was assumed that the soil properties were similar to the layer immediately below. The properties of the embankment surcharge (E = 5100 kPa, ν = 0.3 and γ = 20.5 kN/m^3), and related shear strength parameters (c' = 19 kPa and ϕ' = 26°), were obtained from drained tri-axial tests.

The finite element discretisation is shown by Fig. 10. The embankment was constructed at a rate of 0.4 m/week. Instruments such as inclinometers, piezometers, and settlement plates were installed at this site (Fig. 11).

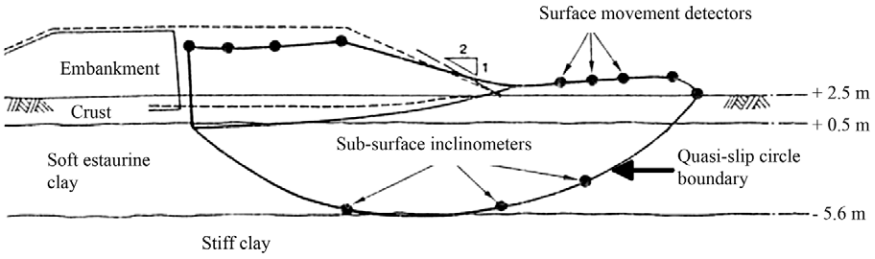

Figure 9 - Failure mode of embankment and foundation (modified after Brand & Premchitt, 1989).

Table 1 - Soil parameters used in the Modified Cam-clay model (CRISP) (Source: Indraratna *et al.*, 1992).

Depth (m)	κ	λ	M	e_{cs}	K_w x 10^4 (cm^2/s)	γ (kN/m^3)	k_h x 10^{-9} (m/s)	k_v x 10^{-9} (m/s)
0-2.0	0.05	0.13	1.19	3.07	4.4	16.5	1.5	0.8
2.0-8.5	0.05	0.13	1.19	3.07	1.1	15.5	1.5	0.8
8.5-18	0.08	0.11	1.07	1.61	22.7	15.5	1.1	0.6
18-22	0.10	0.10	1.04	1.55	26.6	16.1	1.1	0.6

Table 2 - Soil parameters for hyperbolic stress strain model ISBILD (Source: Indraratna *et al.*, 1992).

Depth (m)	K	c_u (kPa)	K_{ur}	c' (kPa)	ϕ' (degree)	γ (kN/m^3)
0-2.5	350	15.4	438	8	6.5	16.5
2.5-8.5	280	13.4	350	22	13.5	15.5
8.5-18.5	354	19.5	443	16	17.0	15.5
18.5-22.5	401	25.9	502	14	21.5	16.0

Note: K and K_{ur} are the modulus number and unloading-reloading modulus number used to evaluate the compression and recompression of the soil, respectively.

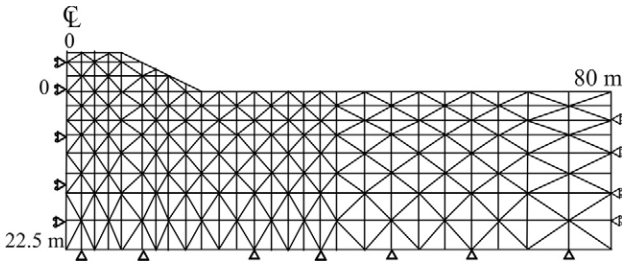

Figure 10 - Finite element discretisation of embankment and subsoils (modified after Indraratna *et al.*, 1992).

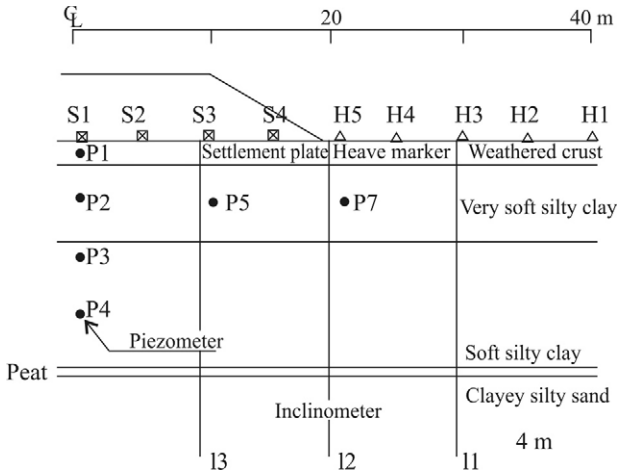

Figure 11 - Cross section of Muar test embankment indicating key instruments (modified after Ratnayake, 1991).

The yielding zones and potential failure surface observed were based on the yielded zone boundaries and maximum displacement vectors obtained from CRISP. Figures 12 and 13 show the shear band predicted, based on the maximum incremental displacement and the boundaries of yielded zone approaching the critical state, respectively. The yielded zone was near the very bottom of the soft clay layer but it eventually spread to the centre line of the embankment, which verified that the actual failure surface was within the predicted shear band.

4.2. Second Bangkok International Airport

The Second Bangkok International Airport or Suvarnabhumi Airport is about 30 km from the city of Bangkok, Thailand. Because the ground water was almost at the surface, the soil suffered from a very high moisture content, high compressibility and very low shear strength. The compression index ($C_c/(1 + e_0)$)varied between 0.2-0.3. The soft estuarine clays in this area often pose problems that require ground improvement techniques before any permanent structures can be constructed.

As reported by AIT (1995), the profile of the subsoil showed a 1 m thick, heavily over-consolidated crust overlying very soft estuarine clay which was approximately 10 m below the bottom of a layer of crust. Approximately 10 to 21 m beneath this crust there was a layer of stiff clay. The ground water level varied from 0.5 to 1.5 m below the sur-

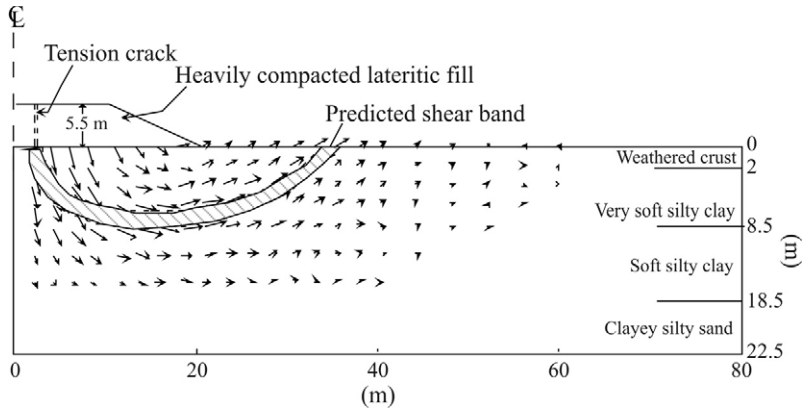

Figure 12 - Maximum incremental development of failure (modified after Indraratna *et al.*, 1992).

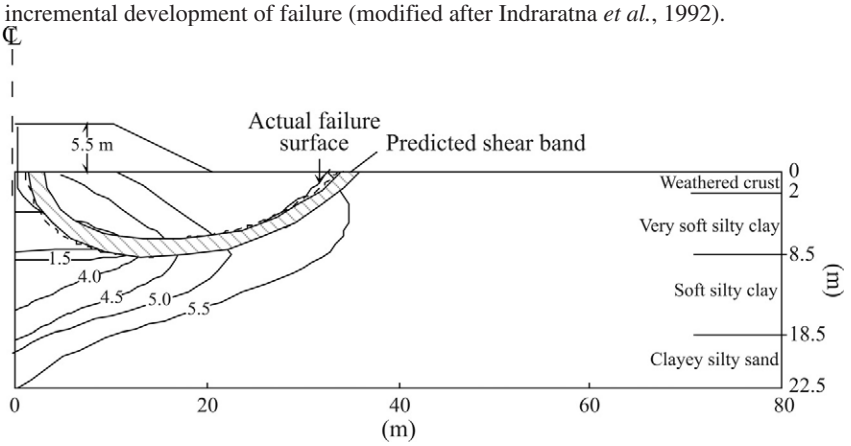

Figure 13 - Boundary zones approaching critical state with increasing fill thickness (CRISP) (modified after Indraratna *et al.*, 1992).

face. The parameters of these layers of subsoil, based on laboratory testing, are given in Table 3.

Two embankments stabilised by vacuum combined with surcharge loading (TV2) and surcharge loading alone (TS1) are described in this section. The performances of embankments TV2 and TS1 were reported by Indraratna & Redana (2000), and Indraratna *et al.* (2005), respectively. The vertical cross section of Embankment TS1 is shown in Fig. 14. TS1 was constructed in multi-stages, with 12 m long PVDs @ 1.5 m in a square pattern. The embankment was 4.2 m high with a 3H:1V side slope. Embankment TV2 was stabilised with vacuum combined surcharge and 12 m long PVDs. A membrane system was also used on this site.

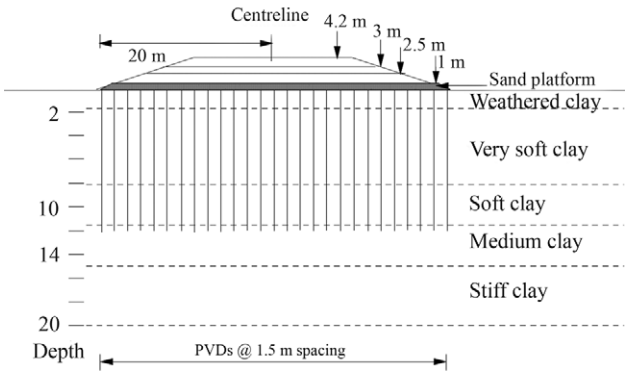

Figure 14 - Cross section at embankment TS1 (After Indraratna & Redana, 2000).

Both embankments were analysed using the finite element software ABAQUS. The equivalent plane strain model (Eqs. (7)-(10)) and modified Cam-clay theory were incorporated into this analysis. The comparisons of the degree of consolidation based on settlement from the FEM and field measurement at the centre line of the embankment are presented in Fig. 15. It can be seen that the application of vacuum pressure reduced the time from 400 to 120 days to achieve the desired degree of consolidation. Figure 16 shows the time dependent excess pore water pressure during consolidation. The vacuum loading generated negative excess pore pressure in TV2 whereas the surcharge fill in embankment TS1 created a positive excess pore pressure. These predicted excess pore pressures agreed with the field measurements. The maximum negative excess pore pressure was approximately 40 kPa, probably caused by a puncture in the membrane and subsequent loss of air. The total applies stresses for both embankment were very similar and therefore yielded similar ultimate settlements (90 cm). The reduction in negative pore pressure at various times was caused by the vacuum being lowered. Despite these problems the analysis using the proposed conversion procedure, including the smear effects, could generally predict the field data quite accurately.

4.3. Sandgate railway embankment

Under railway tracks where the load distribution from freight trains is typically kept below 7-8 m from the surface,

Table 3 - Selected soil parameters in FEM analysis (Indraratna *et al.* 2005).

Depth (m)	λ	κ	ν	k_v 10^{-9} m/s	k_h 10^{-9} m/s	k_s 10^{-9} m/s	k_{hp} 10^{-9} m/s	k_{sp} 10^{-9} m/s
0.0-2.0	0.3	0.03	0.30	15.1	30.1	89.8	6.8	3.45
2.0-8.5	0.7	0.08	0.30	6.4	12.7	38.0	2.9	1.46
8.5-10.5	0.5	0.05	0.25	3.0	6.0	18.0	1.4	0.69
10.5-13	0.3	0.03	0.25	1.3	2.6	7.6	0.6	0.30
13.0-15	1.2	0.10	0.25	0.3	0.6	1.8	0.1	0.07

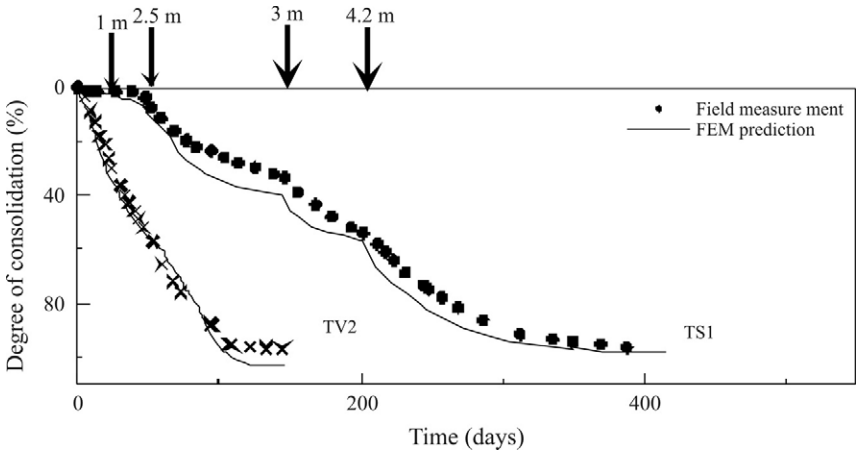

Figure 15 - Degree of Consolidation at the centreline for embankments (after Indraratna & Redana, 2000 and Indraratna *et al.*, 2005).

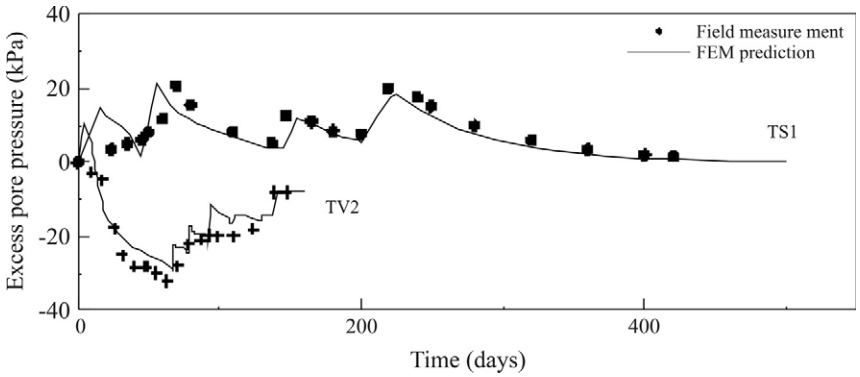

Figure 16 - Excess pore pressure variation at 5.5 m depth (after Indraratna & Redana, 2000 and Indraratna *et al.*, 2005).

relatively short PVDs may still dissipate cyclic pore pressures and curtail any lateral movement of the soft formation. It was expected that any excessive settlement of deep estuarine deposits during the initial stage of consolidation may compensate for continuous ballast packing. However, the settlement rate can still be controlled by optimising the spacing and pattern of drain installation. In this section a case history where short PVDs were installed beneath a rail track built on soft formation is presented with the finite element analysis (Indraratna *et al.* 2010). The finite element analysis used by the Authors to design the track was a typical Class A prediction for a field observation because it was made before it was constructed.

To improve the conditions for rail traffic entering Sandgate, Kooragang Island, Australia, where major coal mining sites are located, two new railway lines were needed close to the existing track. An in-situ and laboratory test was undertaken by GHD Longmac (Chan, 2005) to obtain the essential soil parameters. This investigation included boreholes, piezocone tests, in-situ vane shear tests, test pits, and laboratory tests that included testing the soil index property, standard oedometer testing, and vane shear testing.

The existing embankment fill at this site overlies soft compressible soil from 4 to 30 m deep over a layer of shale bedrock. The properties of this soil, with depth, are shown in Fig. 17, where the groundwater level was at the surface. Short, 8 m long PVDs were used to dissipate excess pore pressure and curtail lateral displacement. There was no preloading surcharge embankment provided due to stringent time commitments. The short PVDs were only expected to consolidate a relatively shallow depth of soil beneath the track where it would be affected by the train load. This initial load was considered to be the only external surcharge. An equivalent static approach based on the dynamic impact factor was used to simulate the field conditions, in this instance a static load of 80 kPa and an impact factor of 1.3 in conjunction with a speed of 40 km/h and a 25 tonne axle load. The Soft Soil model and Mohr-Coulomb model incorporated into the finite element code PLAXIS, were used in this analysis (Brinkgreve, 2002). Figure 18 illustrates a cross-section of the rail track formation.

In the field the 8 m long PVDs were spaced at 3 m intervals, based on the Authors' analysis and recommendations. Figures 19 and 20 show a comparison between the predicted and measured settlement at the centre line of the

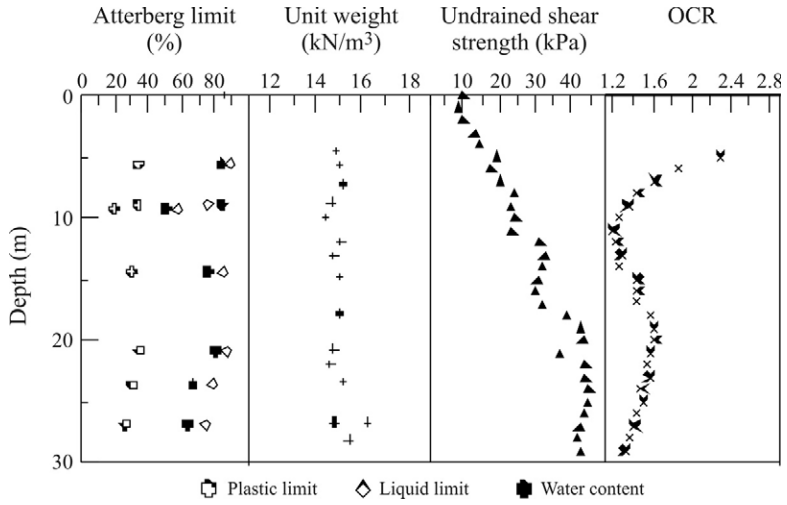

Figure 17 - Soil properties at Sandgate Rail Grade Separation Project (adopted from Indraratna *et al.* 2010).

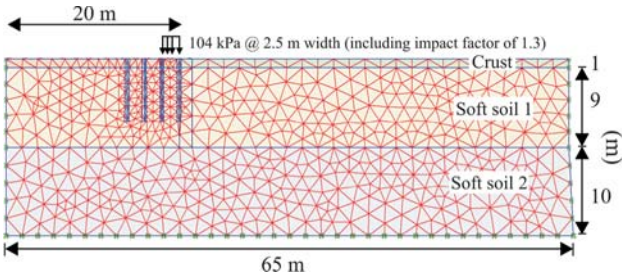

Figure 18 - Vertical cross section of rail track foundation (after Indraratna *et al.* 2010).

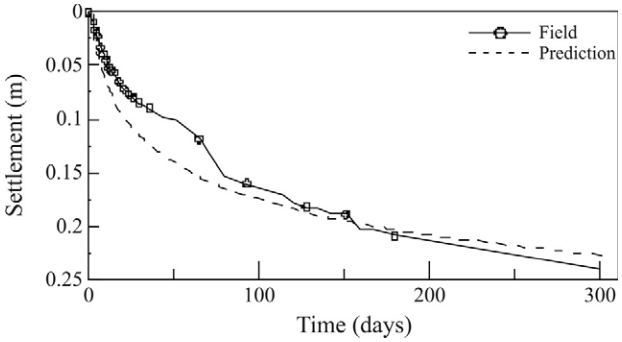

Figure 19 - Predicted and measured at the centre line of rail tracks (after Indraratna *et al.* 2010).

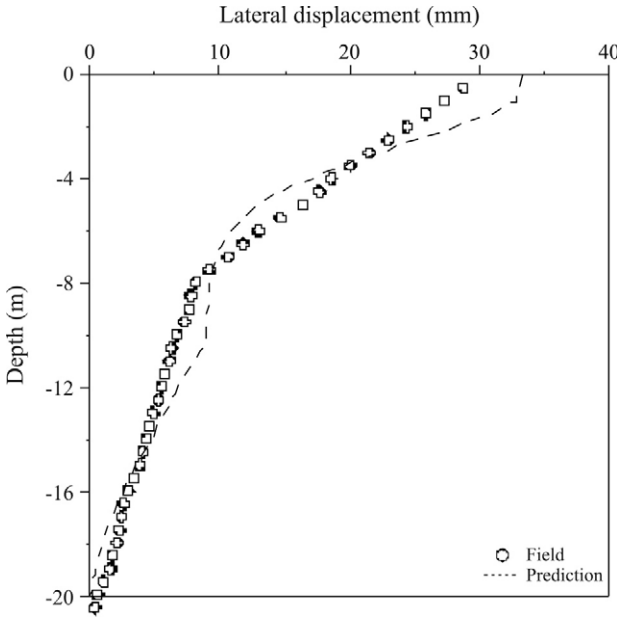

Figure 20 - Measured and predicted lateral displacement profiles near the rail embankment toe at 180 days (after Indraratna *et al.* 2010).

rail track and lateral displacement after 180 days, respectively. The predicted settlement agreed with the field data for a Class A prediction, with the maximum displacement being contained within the top layer of clay. The "Class A" prediction of lateral displacement agreed with what occurred in the field.

5. Conclusion

Various types of vertical drains have been used to accelerate the rate of primary consolidation. A comparison between embankments stabilised with a vacuum combined with a surcharge, and a surcharge alone, were analysed and discussed. Consolidation time with a vacuum applied was substantially reduced and lateral displacement curtailed, and if sufficient vacuum pressure is sustained, the thickness of the surcharge fill required may be reduced by several metres.

A plane strain finite element analysis with an appropriate conversion procedure is often enough to obtain an accurate prediction for large construction sites. An equivalent plane strain solution was used for selected case histories to demonstrate its ability to predict realistic behaviour. There is no doubt that a system of vacuum consolidation via PVDs is a useful and practical approach for accelerating radial consolidation because it eliminates the need for a large amount of good quality surcharge material, via air leak protection in the field. Accurate modelling of vacuum preloading requires both laboratory and field studies to quantify the nature of its distribution within a given formation and drainage system.

It was shown from the Sandgate case study that PVDs can decrease the buildup of excess pore water pressure during cyclic loading from passing trains. Moreover, during rest periods PVDs continue to simultaneously dissipate excess pore water pressure and strengthen the track. The predictions and field data confirmed that lateral displacement can be curtailed which proved that PVDs can minimize the risk of undrained failure due to excess pore pressure generated by cyclic train loads.

Acknowledgments

The authors appreciate the support given by the Australian Rail Track Corporation (ARTC), and John Holland Pty Ltd. They wish to thank the CRC for Rail Innovation (Australia) for its continuous support. The embankment data provided by the Asian Institute of Technology are appreciated. A number of other current and past doctoral students, namely, Mr. Somalingam Balachandran, Ms. Pushpachandra Ratnayake, Dr. I Wayan Redana, Dr. Chamari Bamunawita, Dr. Iyathurai Sathananthan, Dr. Rohan Walker, and Mr. Ali Ghandeharioon also contributed to the contents of this keynote paper. More elaborate details of the contents discussed in this paper can be found in previous publications of the first author and his research students in Geotechnique, ASCE, Canadian Geotechnical Journals, since mid 1990's and Dr. Rujikiatkamjorn PhD thesis for the work related to Bangkok case histories.

References

AIT (1995) The Full Scale Field Test of Prefabricated Vertical Drains for The Second Bangkok International Airport (SBIA). AIT, Bangkok, 259 pp.

Atkinson, M.S. & Eldred, P. (1981) Consolidation of soil using vertical drains. Geotechnique, v. 31:1, p. 33-43.

Barron, R.A. (1948) Consolidation of fine-grained soils by drain wells. Transactions ASCE, v. 113, p. 718-724.

Brand, E.W. & Premchitt, J. (1989) Moderator's report for the predicted performance of the Muar test embankment. Proc. International Symposium on Trial Embankment on Malysian Marine Clays, Kuala Lumpur, v. 2, pp. 1/32-1/49.

Brinkgreve, R.B.J. (2002) PLAXIS (Version 8) User's Manual. Delft University of Technology and PLAXIS B.V., Netherlands, 162 pp.

Cao, L.F.; Teh, C.I. & Chang, M.F. (2001) Undrained cavity expansion in modified cam clay I: Theoretical analysis. Geotechnique, v. 51:4, p. 323-334.

Chan, K. (2005) Geotechnical Information Report for the Sandgate Rail Grade Separation, Hunter Valley Region. Australia, 67 pp.

Cognon, J.M.; Juran, I. & Thevanayagam, S. (1994) Vacuum consolidation technology-principles and field experience. Proc. Conference on Foundations and Embankments Deformations, College Station, Texas, v. 2, pp. 1237-1248.

Ghandeharioon, A.; Indraratna, B. & Rujikiatkamjorn, C. (2009) Analysis of soil disturbance associated with mandrel-driven prefabricated vertical drains using an elliptical cavity expansion theory. International Journal of Geomechanics, ASCE, v.20:2, p. 53-64.

Hansbo, S. (1979) Conslidation of clay by band-shaped prefabricated drains. Ground Eng., v. 12:5, p. 16-25.

Hansbo, S. (1981) Consolidation of fine-grained soils by prefabricated drains. Proceedings of 10th International Conference on Soil Mechanics and Foundation Engineering, Stockholm, Balkema, v. 3, pp. 677-682.

Hird, C.C.; Pyrah, I.C. & Russell, D. (1992) Finite element modelling of vertical drains beneath embankments on soft ground. Geotechnique, v. 42:3, p. 499-511.

Holtz, R.D. (1987) Preloading with prefabricated vertical strip drains. Geotextiles and Geomembranes, v. 6(1-3), p. 109-131.

Indraratna, B. & Redana, I.W. (2000) Numerical modeling of vertical drains with smear and well resistance installed in soft clay. Canadian Geotechnical Journal, v. 37:1, p. 132-145.

Indraratna, B.; Bamunawita, C. & Khabbaz, H. (2004) Numerical modeling of vacuum preloading and field applications. Canadian Geotechnical Journal, v. 41:6, p. 1098-1110.

Indraratna, B.; Balasubramaniam, A.S. & Balachandran, S. (1992) Performance of test embankment constructed to failure on soft marine clay. Journal of Geotechnical Engineering, ASCE, v. 118:1, p. 12-33.

Indraratna, B.; Balasubramaniam, A.S. & Ratnayake, P. (1994) Performance of embankment stabilized with vertical drains on soft clay. J. Geotech. Eng., ASCE, v. 120:2, p. 257-273.

Indraratna, B.; Balasubramaniam, A.S. & Sivaneswaran, N. (1997) Analysis of settlement and lateral deformation of soft clay foundation beneath two full-scale embankments. International Journal for Numerical and Analytical Methods in Geomechanics, v. 21:9, p. 599-618.

Indraratna, B.; Rujikiatkamjorn C. & Sathananthan, I. (2005) Analytical and numerical solutions for a single vertical drain including the effects of vacuum preloading. Canadian Geotechnical Journal, v. 42:4, p. 994-1014.

Indraratna, B. & Rujikiatkamjorn, C. (2008) Effects of partially penetrating prefabricated vertical drains and loading patterns on vacuum consolidation. In: K.R. Reddy, M.V. Khire and A.N. Alshawabkeh (eds), GeoCongress, ASCE, pp. 596-603.

Indraratna, B.; Rujikiatkamjorn, C.; Adams, M. & Ewers, B. (2010) Class A prediction of the behaviour of soft estuarine soil foundation stabilised by short vertical drains beneath a rail track. International Journal of Geotechnical and Geo-environmental Engineering, ASCE, v. 136:5, p. 686-696.

Kjellman, W. (1948) Accelerating consolidation of fine grain soils by means of cardboard wicks. Proc. 2nd ICSMFE, Rotterdam, v. 2, pp. 302-305.

Li, A.L. & Rowe, R.K. (2002) Combined effect of reinforcement and prefabricated vertical drains on embankment performance. Canadian Geotechnical Journal, v. 38:6, p. 1266-1282.

Long, R. & Covo, A. (1994) Equivalent diameter of vertical drains with an oblong cross section. Journal of Geotechnical Engineering, v. 20:9, p. 1625-1630.

Ozawa, Y. & Duncan, J.M. (1973) ISBILD: A Computer Program for Static Analysis of Static Stresses and Movement in Embankment. University of California, Berkeley, 144 pp.

Ratnayake, A.M.P. (1991) Performance of test embankments with and without vertical drains at Muar flats site, Malaysia. Master Thesis, GT90-6, Asian Institute of Technology, Bangkok, 190 pp.

Sathananthan, I. & Indraratna, B. (2006) Laboratory evaluation of smear zone and correlation between permeability and moisture content. J. of Geotechnical & Geoenvironmental Engineering, ASCE, v. 132:7, p. 942-945.

Sathananthan, I.; Indraratna, B. & Rujikiatkamjorn C., (2008) The evaluation of smear zone extent surrounding mandrel driven vertical drains using the cavity expansion theory. International Journal of Geomechanics, ASCE, v. 8:6, p. 355-365.

Woods, R. (1992) SAGE CRISP Technical Reference Manual. The CRISP Consortium Ltd., Cambridge, 223 pp.

Yoshikuni, H. & Nakanodo, H. (1974) Consolidation of fine-grained soils by drain wells with finite permeability. Japanese Society Soil Mechanics and Foundation Engineering, v. 14:2, p. 35-46.